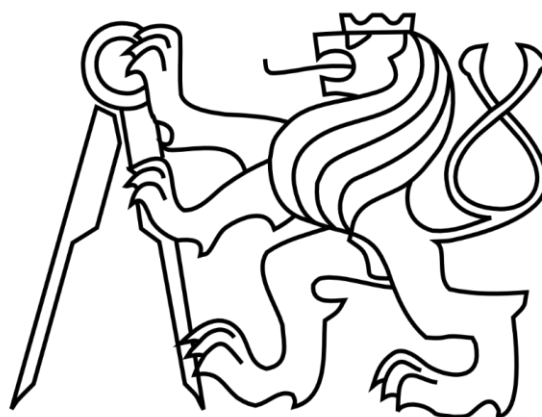CZECH TECHNICAL UNIVERSITY IN PRAGUE

FACULTY OF ELECTRICAL ENGINEERING
DEPARTMENT OF POWER ENGINEERING

Master's Thesis

Advanced methods of fault localization on HV lines
Pokročilé metody lokalizace poruch na VN vedeních

Author: Nikola Miljkovic

Study Program: Electrical Engineering, Power Engineering and
Management

Supervisor: doc. Dr. Ing. Jan Kyncl

MASTER'S THESIS ASSIGNMENT

I. Personal and study details

Student's name: **Miljkovic Nikola** Personal ID number: **462262**

Faculty / Institute: **Faculty of Electrical Engineering**

Department / Institute: **Department of Electrical Power Engineering**

Study program: **Electrical Engineering, Power Engineering and Management**

Specialisation: **Electrical Power Engineering**

II. Master's thesis details

Master's thesis title in English:

Advanced methods of fault localization on HV lines

Master's thesis title in Czech:

Advanced methods of fault localization on HV lines

Guidelines:

1. Understand the types of faults on the lines
2. Describe the current state of fault location on lines
3. Describe the method of locating faults on lines using H matrices
4. Carry out a case study using H matrices to locate faults on lines

Bibliography / sources:

1. C37.114-2014 - IEEE Guide for Determining Fault Location on AC Transmission and
2. Distribution Lines
10.1109/TENCON.2009.5396253 Impedance-based fault location techniques for transmission lines

Name and workplace of master's thesis supervisor:

doc. Dr. Ing. Jan Kyncl, Department of Electrical Power Engineering, FEE

Name and workplace of second master's thesis supervisor or consultant:

Date of master's thesis assignment: **19.02.2020** Deadline for master's thesis submission: _____

Assignment valid until: **19.02.2022**

_____ _____ _____
doc. Dr. Ing. Jan Kyncl Head of department's signature prof. Mgr. Petr Páta, Ph.D.
Supervisor's signature Dean's signature

III. Assignment receipt

The student acknowledges that the master's thesis is an individual work. The student must produce his thesis without the assistance of others, with the exception of provided consultations. Within the master's thesis, the author must state the names of consultants and include a list of references.

_____ _____
Date of assignment receipt Student's signature

Declaration

I hereby declare that this thesis is the result of my own work and all the sources I used in the list of references, in accordance with the Methodological Instructions of Ethical Principle in the preparation of University thesis.

In Prague 21.05.2018   N.Miljkovic signature:………………….

Acknowledgement

Abstract

Transmission line networks are becoming less linear and more meshed as time goes on. New algorithms for fault localization are needed to cater for the increasing complexity of line networks. A progressive algorithm using H matrices was described in this thesis. The algorithm and simulation of lines were realized using Mathematica® version 12. The types of faults that overhead lines have, their parameters and how to localize those faults were described first. The progressive algorithm used to localize the faults was analysed for all different types of faults. Accuracy of the algorithm was tested in different locations of faults. Influences of total vector error for the phasors used to calculate the H-matrix were examined.

Keywords: Overhead lines, localization, fault, synchrophasors, Mathematica, high voltage, transmission, algorithm, H matrix.

Abstraktní

Síť přenosových vedení se postupem času stává méně jednorozměrnou a více propojenou. Nové algoritmy pro lokalizaci poruch mohou pomoci zabezspečit provoz při rostoucí složitosti sítí. V této práci byl popsán progresivní algoritmus využívající H matice. Algoritmus a simulace linek byly realizovány pomocí Mathematica® verze 12. Nejprve byly popsány typy poruch, které se mohou přihodit na vedeních, parametry vedení a způsoby tyto poruchy lokalizovat. Navrhovaný algoritmus používaný k lokalizaci poruch byl analyzován většinu možných typů poruch. Přesnost algoritmu byla testována pro různá místa poruchy. Byly zkoumány vlivy chyb pro fázorů použitých pro výpočet H-matic.

Klíčová slova: Přenosové vedení, lokalizace, porucha, synchrofázory, Mathematica, vysoké napětí, přenos, algoritmus, H matice.

Table of Contents

Table of Figures

Table of tables

1. Introduction

Overhead line faults are a major factor in transmission and distribution grid reliability and quality. While good planning and testing can decrease the amount of faults occurring significantly, it can never fully remove random faults or faults due to external factors. With overhead lines potentially being hundreds of kilometres long and faults occurring at random location and time, extensive work is required for localization and diagnostics of faults.

Concurrent devices for fault localization only take into impedance values of the line and compare them with reference values. While this method is accurate enough on simple overhead line schematics and configurations, with the ever increasing complexity of today's grids the method is found lacking. A progressive algorithm is proposed with the ability to keep up with the more complex grid schematics and specifications, which will allow transmission operators to more efficiently locate and diagnose faults which in turn leads to less downtime.

The progressive algorithm works on the principles of the H-matrix which takes into account not only the impedance characteristics but also the self and mutual inductances, the types of conductor arrangements as well as parallel lines (even when unsymmetrical).

2. Overhead line faults

A fault occurring causes high currents to travel through the conductor, these high currents can lead to high temperatures in the conductors for which they were not designed for as well as causing instabilities in the voltage which can damage equipment [2]. Protection equipment must be carefully selected to cut the time of the fault down to as small as possible.

Transmission line faults can be quantified in many ways. The simplest form is symmetrical and asymmetrical faults. Symmetrical faults are comprised of a three-phase short circuit fault which means that each phase has an equal amount of variation from the reference values. Asymmetrical faults are comprised by phase-to-ground, phase-to-phase and double-phase-to-ground faults. These faults have uneven currents in between the phases due to their nature. All 4 types of faults are described schematically in figs. 2.1-4. An important design note on protection systems is that symmetrical faults usually have the smallest short-circuit currents and therefore are not suitable for choosing protection equipment based on the currents these faults provide but rather a study should be done to find the highest short-circuit current and chose equipment based on that value.

Another type of classification of faults is the cause of the faults such as: tree, lightning, insulator degradation, accident…etc. These classifications are mostly used to study fault occurrence and to try preventing the types of faults from occurring.

In transmission lines the most frequent type of fault is phase-to-ground (~93%), followed by double-phase-to-ground (~5%) and the other two faults (phase-to-phase and three-phase) with very low occurrences (~1%) each [10].
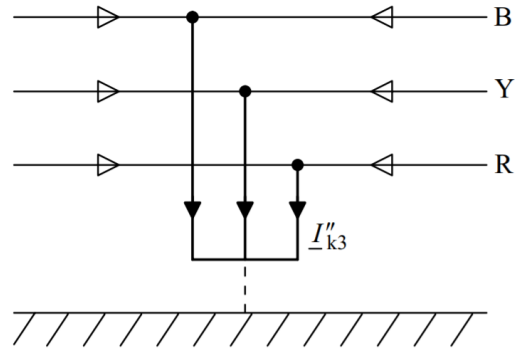
Fig.2.1. Three-phase
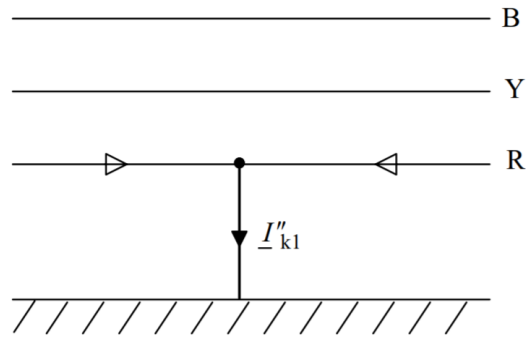
Fig.2.2 Phase-to-ground fault
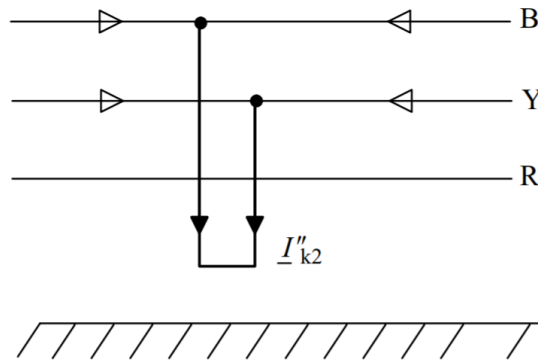
Fig.2.3. Phase-to-Phase fault
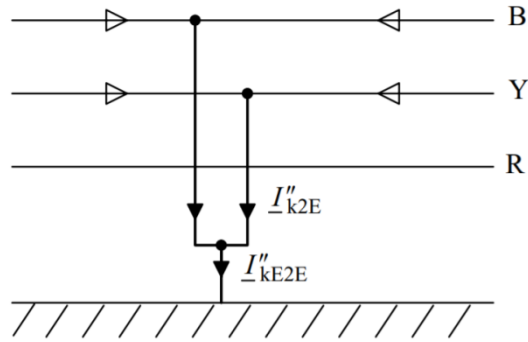
Fig.2.4 Double-phase-to-ground fault

Where the arrows along the phases B-Y-R indicate a-c current flow and $I\overset{``}{\phantom{}}_3$, $I\overset{``}{}_2$, $I\overset{``}{\phantom{}}$ ,$I\overset{``}{}_{k2E}$ are all respective short-circuit currents.

3. Overhead line parameters

Accurate mathematical representation of overhead line parameters is essential for building a progressive algorithm that will be able to accurately represent the real life equipment and their specifications. The model for an overhead line takes into account the series resistance and inductance and the shunt capacitance and conductance. Overhead lines have the 4 mentioned parameters proportional to their length. Therefore to model the overhead line we must consider these parameters as per unit length or per kilometre (km).

Rdx – resistance per kilometre $(\frac{\Omega}{Km})$

Xdx – inductance per kilometre $(\frac{L}{Km})$

Cdx – capacitance per kilometre $(\frac{C}{Km})$

Gdx – conductance per kilometre $(\frac{S}{Km})$
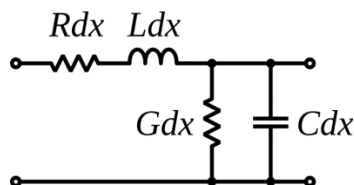
Fig.3.1 Overhead line parameters per unit length

These parameters can be modelled as lumped parameters in different ways, π and T models are the most common. The models are shown in the figs.3.2-3below.
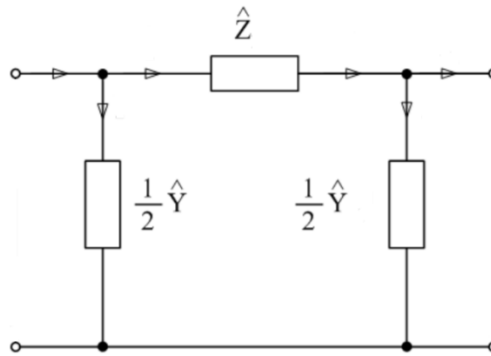
Fig.3.2. π model of transmission line
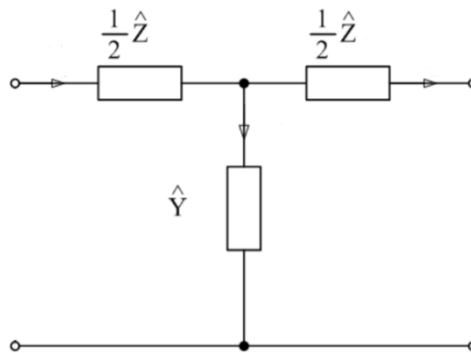
Fig.3.3. T model of transmission line

With the following formulas explaining the relationship of the former simple model with the lumped parameters models:

$$Z = R + jX = Rdx * D + jXdx * D \quad (3.1)$$

$$Y = G + jC = Gdx * D + Cdx * D \quad (3.2)$$

Where Z is impedance (Ω), Y is admittance (S), D is length of overhead line (m), R is resistance (Ω), X is reactance (L), G is conductance (S) and C is capacitance (C).

4. Protection systems and apparatus

Protection systems are crucial transmission apparatuses as they protect grids equipment from additional damage that can be caused by faults. Protection systems must disconnect faulty sections of the grid as soon as possible to prevent: overheating of the conductors by short-circuit currents, non-nominal voltage levels and unbalanced three phase operation. This means that the protection system must be able to detect these fault conditions and act appropriately.

4.1 Instrument transformer

Detection and monitoring is done by instrument transformers. There are two types of such transformers: current type and potential type. The potential type in turn then can be separated into 3 more types: electromagnetic, capacitive and optical. Instrument transformers must have as little a load as possible on the phase conductors while accurately measuring the voltage or current from that same phase. Instrument transformers used in protection systems are usually connected to monitoring systems, protections relays or both in the secondary winding.

Current type instrument transformers step down the current in the measured conductor to a more suitable level for measuring, to do this the transformer has very few turns in the primary side but a large number of turns in the secondary side where the ammeter is directly connected. On the other hand voltage types, while also a stepping down the voltage, have large number of turns in the primary and a few number of turns in the secondary where the voltmeter is directly connected. The difference is due to the different impedances of the voltmeter and ammeter.

4.2 Protection relay

A protection relay is a device that opens or closes segments of the transmission system in abnormal conditions such as faults. Protection relays are classified in two groups: measuring and all-or-nothing relays. Measuring relays are triggered to turn on or off by certain values of current, voltage, power or phase. In turn all-or-nothing relays do not have a setting and are energized by certain quantity, when this quantity is too high or too low the relay switches on or off. All-or-nothing relays are rarely used nowadays with their inability to be adjusted [2].

Measuring relays are triggered by a various amount of measured quantities such as:

- Current relays: Operate at a predetermined threshold value of current.
- Voltage relays: Operate at a predetermined value of voltage.
- Power relays: Operate at a predetermined value of power.
- Differential relays: Operate according to the scalar or vectorial difference between two quantities such as current, voltage, etc.
- Distance relays: Operate according to the "distance" between the relay's current transformer and the fault. The "distance" is measured in terms of resistance, reactance, or impedance.

4.3 Distance protection relay

Distance protection relay is an impedance based type of protection where the relay measures impedance using a two-input relay comparator. While there are other methods of impedance based protection they usually require measurements of voltage and current from both the ends of the line, this becomes uneconomical in regards to big interconnected grids, unlike the distance protection relay which only needs measurement from one end.

A two-input relay comparator will have one input current proportional to the fault current while the other will be proportional to the fault loop voltage. This means that the impedance of the fault is calculated from these two values, this impedance is then compared to the nominal impedance. If the line impedance was found to be smaller than the nominal impedance then the comparator would trigger the distance protection relay. A mho relay is usually used in practise nowadays as it is naturally directional and has suitable settings that can be calibrated.

Distance protection relays are a stepped type of protection, meaning there is discrete difference in the time of triggering which depends on the distance. Current practise sets the relay to trigger in the same time delay for the first 80-90% of the first section of the feeder line. Then for the second section a 0.5-1 second delay is added. The second section overlaps another distance protection relay for at least an additional 20-50% of its first section i.e. 120-150% from the beginning of the line. The third section has an additional 0.5-1 second delay added to its trigger time and also the relay overlaps the second distance protection relay by an additional 20-50% i.e. 220-250% from the beginning of the line. This characteristic is graphically explained in the fig.4.1. The reason for the staggered overlapping zones is for backup protection.

By changing the characteristics of the mho relay the measured distance of the protection relay is changed. This is graphically represented in fig.4.2.

The distance protection relay can not only locate the fault in one of the three zones but also determine the type of fault. This is done by having additional mho relays for each zone with different characteristics on their respective PT (potential type) and CT (current type) transformers. This option obviously increases costs drastically.
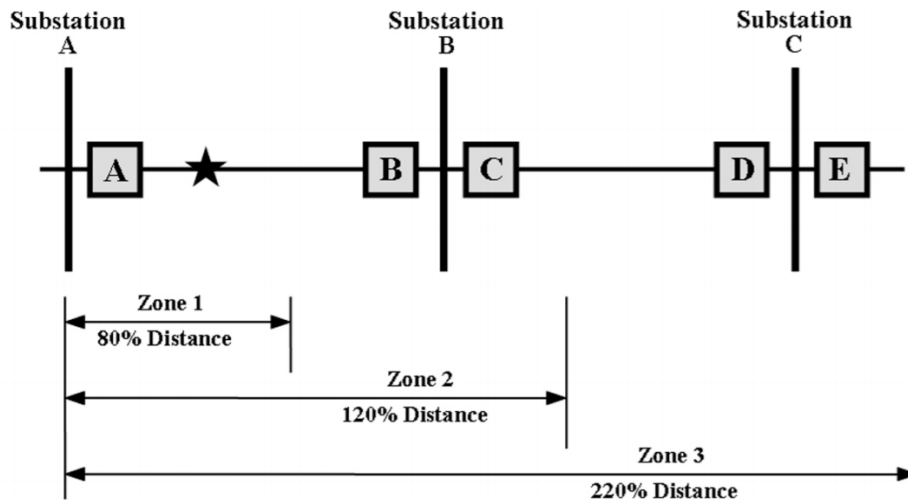
Fig.4.1. Time-distance characteristics of distance protection [3]
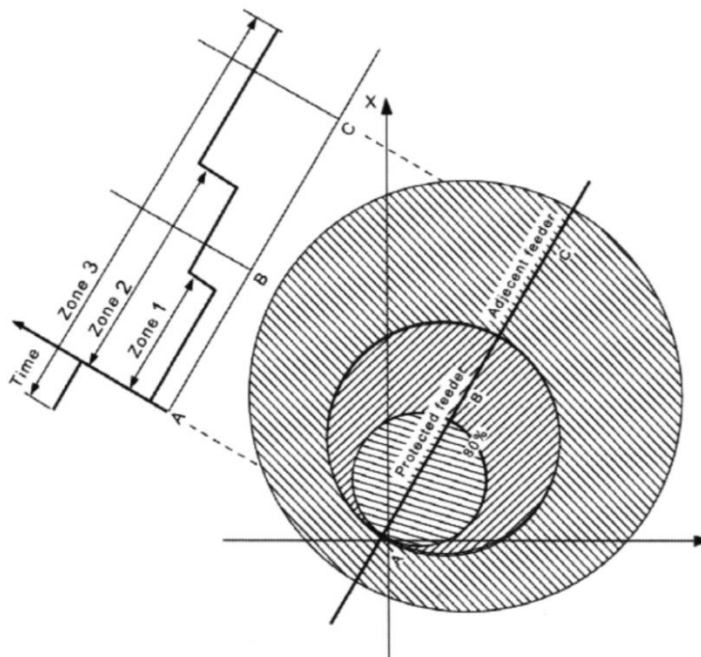
Fig.4.2. Characteristics of a Three-Zone Offset Mho-Relaying Scheme. [2

5. Synchrophasor standards

Synchrophasors standards define inputs and outputs for protective equipment used in power energy such as protection equipment and measuring relays, usually referred to as PMU (phasor measurement unit). The standard defines voltage and current synchronized phasors (synchrophasors) as well as frequency and rate of change of frequency (ROCOF). Also it describes the conditions needed to synchronize and time tag the three types of data provided [4]. The standardization of these values is

crucial when dealing with cross-country power energy connections as well as connections between different transmission/distribution companies, as difference in standards may result in problems. IEEE has developed a standard for just this purpose, called the C37.118 standard.

This standard defines the accuracy of the voltage and current phasors as well as the reliability of the time input. The PMU that are used in power electronics must follow these accuracies. In Fig.5.1 you can see the visual representation of the input and output expectations of the standard.
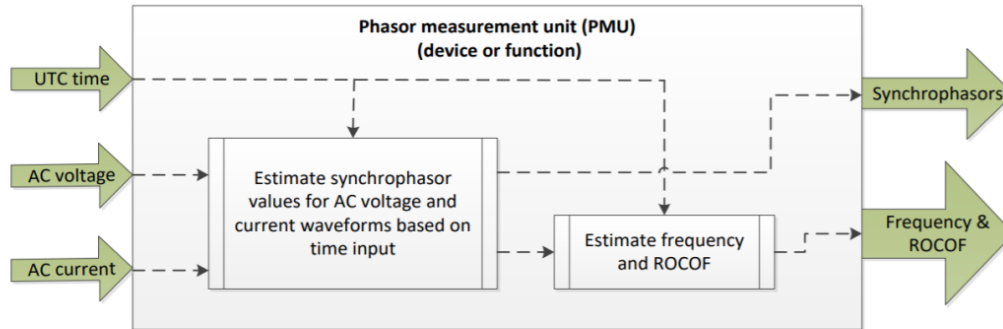
Fig.5.1. description of expected inputs and outputs for a PMU [4]

Measurement time synchronization

UTC time input must be from a reliable and accurate source such as global navigation satellite system. The UTC time input has an important job of synchronizing all the other inputs/outputs so slight deviations of errors can lead to serious issues. A phase error of 0.01 radian or 0.057^o will cause a 1% TVE (total vector error). TVE will be defined later in this chapter (equation 5.7). 1% is the maximum allowed error with regard the time input. This corresponds to a time error of $\pm$ 26 µs for a 60 Hz system, and $\pm$ 31 µs for a 50 Hz system [4]. It is recommended that time input has 10 times better accuracy than that which creates 1% TVE. Each output will be time tagged using the UTC time input with a 1µs precision.

Synchrophasors

The voltage or current in an AC power grid is modelled with the following equation:

$$(t) = X\mathrm{m}(t)\cos[\theta(t)] + D(t) \qquad (5.1)$$

where t is time in seconds, where t = 0 is coincident with a UTC second rollover; Xm is the peak magnitude of the sinusoidal AC signal; θ is the angular position of the sinusoidal AC signal in radians; D is a disturbance signal that contains additive contributions to the signal, including, but not limited to harmonics, noise, DC offset and out-of-band interference.

The synchrophasor phase angle $\phi(t)$ is defined as the phase difference between the angular position $\theta(t)$ and phase due to the nominal frequency f_0:

$$\phi(t) = \theta(t) - 2\pi f_0 \qquad (5.2)$$

The phasors for current and voltage can be expressed in two different ways, as polar coordinates:

$$X(t) = \left(\frac{Xm(t)}{\sqrt{2}}, \phi(t)\right) \qquad (5.3)$$

Or alternatively as real and complex components:

$$X_R(t) = \left(\frac{Xm(t)}{\sqrt{2}} \cos[\phi(t)]\right) \qquad (5.4)$$

$$X_I(t) = \left(\frac{Xm(t)}{\sqrt{2}} \sin[\phi(t)]\right) \qquad (5.5)$$

Where $X_R(t)$ is the real component, $X_I(t)$ is the imaginary component, $Xm(t)$ is the peak amplitude of the signal and $\phi(t)$ is the phase angle.

Rate of change of frequency

The ROCOF measurand is the angular acceleration of the AC power system signal in units of Hz/s. It relates to the angular velocity of the power system signal

$$ROCOF(t) = \frac{df(t)}{dt} = \frac{1}{2\pi}\frac{d^2\theta(t)}{dt^2} = \frac{1}{2\pi}\frac{d^2\phi(t)}{dt^2} \qquad (5.6)$$

TVE (total vector error)

The measurement of the TVE for each of the components in the PMU is very vital for establishing the accuracy limits. The TVE determines the differences between a PMUs estimates of the signal and the reference values calculated according to models provided.

The TVE describes both magnitude and phase angle errors in its calculations. This means that all the possible errors are covered, be it: magnitude error, noise, time un-synchronization and phase difference.

TVE is defined as follows:

$$TVE(n) = \sqrt{\frac{(Y_R(n) - X_R(n))^2 + (Y_I(n) - X_I(n))^2}{X_R(n)^2 + X_I(n)^2}} \qquad (5.7)$$

where $\Upsilon_R(n)$ and $\Upsilon_I(n)$ are the real and imaginary PMU estimates at report time n, $X_R(n)$ and $X_I(n)$ are the real and imaginary reference values at report time n; n is the report number representing the report time (the nth report in a series of discrete reports).

The visual representation of what the TVE measurement means can be seen in the Fig.5.2. The figure depicts a circle drawn at the tip of the phasor with radius 1% of the amplitude of the phasor. The reference phasor would be the line on the circumference of the circle. The angle between the two phasors would be 0.573°.
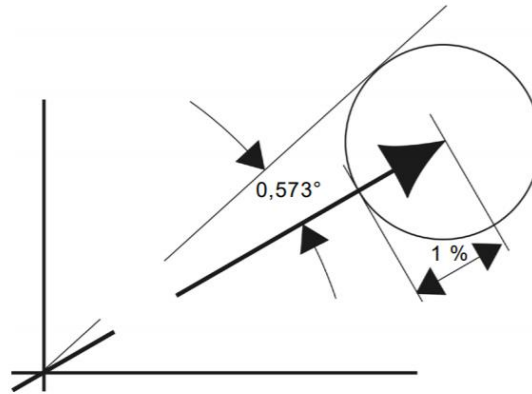
Fig.5.2. Visual representation of TVE

Influence quantity	Reference condition	Minimum range of influence quantity over which PMU shall be within given TVE limit			
		Performance – P class		Performance – M class	
		Range	Max. TVE %	Range	Max. TVE %
Signal frequency	Frequency = f_0 ($f_{nominal}$)	± 2,0 Hz	1	± 2,0 Hz for F_s < 10 ± F_s/5 for 10 ≤ F_s < 25 ± 5,0 Hz for F_s ≥ 25	1
Voltage signal magnitude	100 % rated	80 % to 120 % rated	1	10 % to 120 % rated	1
Current signal magnitude	100 % rated	10 % to 200 % rated	1	10 % to 200 % rated	1
Harmonic distortion (single harmonic)	< 0,2% (THD)	1 %, each harmonic up to 50th	1	10 %, each harmonic up to 50th	1

Table 1. Steady state TVE requirements [4]

Frequency and ROCOF errors

Frequency and ROCOF measurements shall be evaluated as was the TVE by the difference between the measured values provided by the PMU (measured) and the reference values (ref).

Frequency measurement error: $FE(n) = f_{measured}(n) - f_{ref}(n)$ (5.8)

ROCOF error: $RFE(n) = \left(\frac{df_{measured}}{dt}\right)(n) - \left(\frac{df_{ref}}{dt}\right)(n)$ (5.9)

Influence quantity	Reference condition	Error requirements for compliance			
		P class		M class	
Signal frequency	Frequency = f_0 ($f_{nominal}$) Phase angle constant	Range: $f_0 \pm 2{,}0$ Hz		Range: $f_0 \pm 2{,}0$ Hz for $F_s \leq 10$ $\pm F_s/5$ for $10 \leq F_s < 25$ $\pm 5{,}0$ Hz for $F_s \geq 25$	
		Max. |FE|	Max. |RFE|	Max. |FE|	Max. |RFE|
		0,005 Hz	0,4 Hz/s	0,005 Hz	0,1 Hz/s

Table 2. RFE and FE steady state requirements [4] (Where F_s is reporting frequency.)

6. Short-circuit parameters

3-phase a-c short-circuit models must take into consideration two scenarios: "far-from-generator" and "near-to-generator" [5]. Near-to-generator scenario has to take into account short-circuit sub-transient and transient influences from the generator itself. The far-from-generator scenarios do not need to take into account these phenomena as the a-c component of the short circuit stays constant and is not influenced by the changing reactance of the generator.

Short-circuits have a decaying d-c component which is a combination of the reactive and ohmic values coupled with the instant of the short-circuit initiation [6]. This d-c component has to be properly modelled and taken into account when obtaining fault location as it could severely affect the end result.

In Figures 6.1 and 6.2 it is shown the difference between the two scenarios. While the long term short-circuit current might eventually stabilize in both cases it is imperative that the model values fit the real time currents and voltages of the real life scenario.
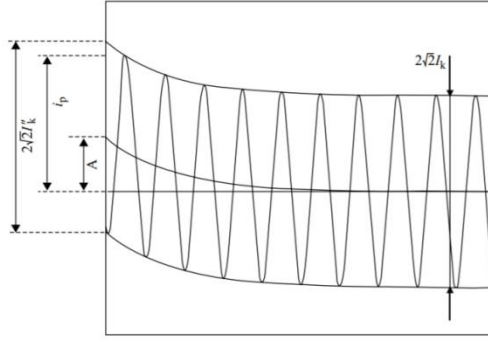
Fig.6.1 Far-from-generator short-circuit [5].
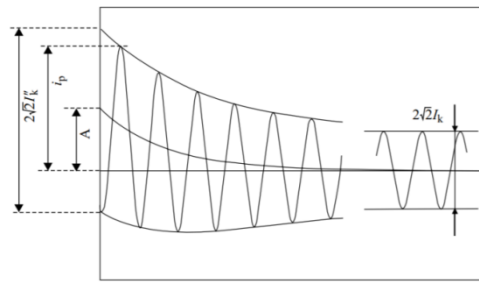
Fig.6.2 Near-of-generator short-circuit [5].

The d-c component is be modelled by:

$$i_{dc} = \sqrt{2} * I_k'' * e^{-2\pi ft*(R/X)} \qquad (6.1)$$

Where I_k'' is the initial symmetrical short-circuit current, f is the power system frequency, t is the time parameter and R, X are the resistance and reactance of the short-circuit impedance [6].

6.1 Goodness-of-fit

The reason for accurate modelling can be explained by comparing the "goodness-of-fit" between the modelled short-circuit and the real time synchrophasors. The goodness-of-fit value is expressed in Decibels [Db] and it is a measurement of the how well the model compares to the synchrophasors [7].

The Goodness-of-fit is evaluated by this equation:

$$GoF = 20\log\frac{X_m}{\sqrt{\frac{1}{(N-m)}\Sigma_{k=1}^{N}(u_k-v_k)^2}} \qquad (6.2)$$

Where N is the number of samples and m is the number of parameters being estimated. The difference N – m indicates the remaining degrees of freedom. X_m is the signal amplitude, u_k is the signal sample value and v_k is the estimated sample value.

This metric evaluates the signals as having a good match when it evaluates +40Dbs while a bad match would have a significantly smaller value such as ~20Dbs.

By the use of real life transient events (short-circuits) and modelled synchrophasors a study on the accuracy of the models can be realized using the G.o.F. metric. The highlight results of such a study can be seen in the fig.6.3 and fig.6.4.
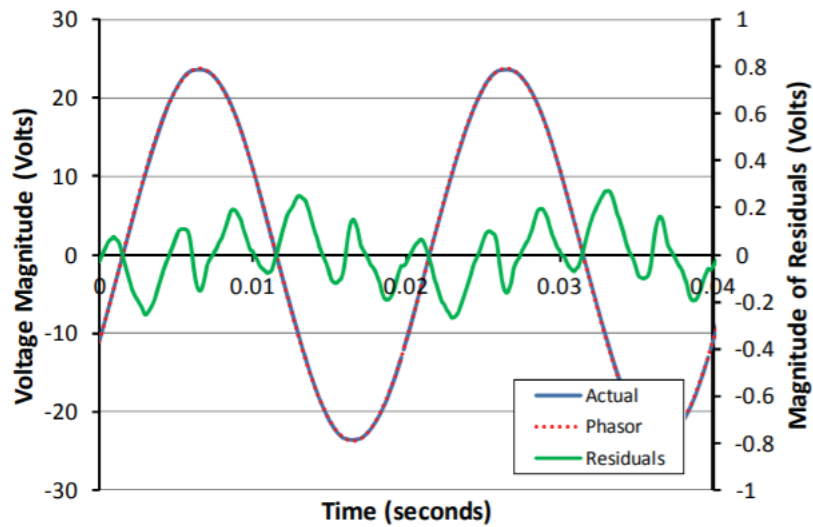
Fig.6.3. The sampled voltage (Actual) is compared to the modelled phasor (phasor) and the difference is calculated (residuals) [7].

Voltage synchrophasors and modelled values, at transient events, seem to have small variances with acceptable levels of difference: pre-transient event (~45Db) and post-transient event (~43Db) G.o.F. values.
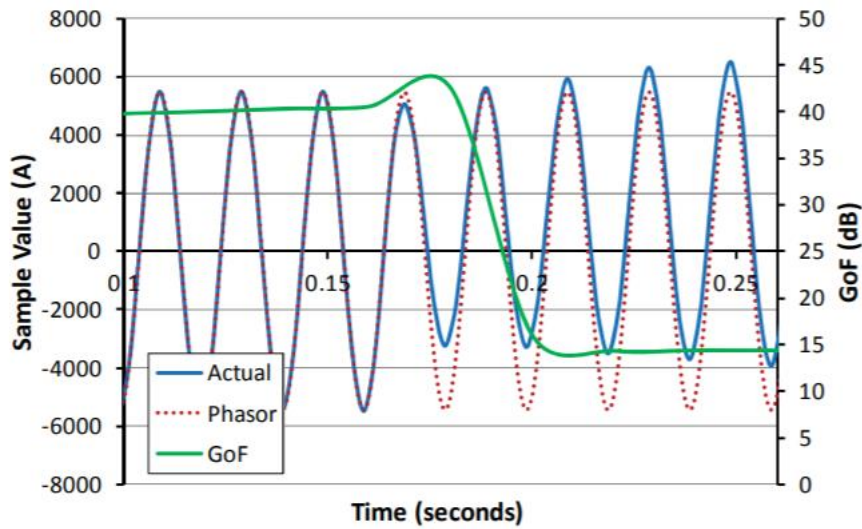
Fig.6.4 The sampled current (Actual) is compared to the modelled phasor (phasor) using the GoF metric [7].

The current synchrophasors show drastic differences with the G.o.F. metric changing from ~40Db to ~15Db [7]. This is most likely due to the d-c component of the current synchrophasor.

7. H-matrix

Fault location has mostly been done by only calculating the impedance of affected lines and then approximating the distance to the fault. In very simple line configurations this could result in acceptable errors, when it came to the actual point of the fault, but when the lines have other influences such as parallel lines or un-transposed lines, the errors would be much greater.

Using H-matrices for fault location can be used to decrease the burden of computing data while at the same time increase accuracy due to the inclusion of mutual effects between the phases and other lines.

7.1 Modelling one phase overhead line with H-matrix

The model used to represent a one phase overhead line is a T-model as discussed in chapter 3.
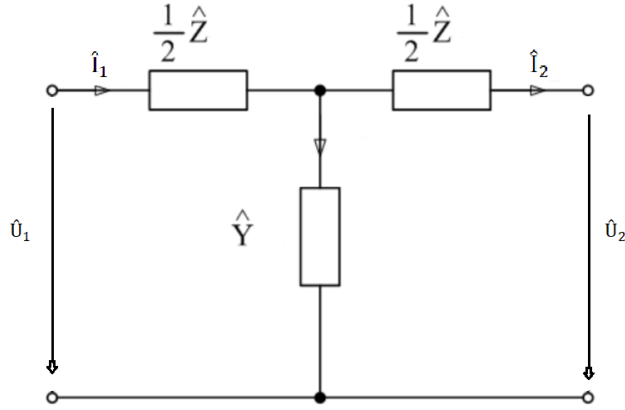
Fig.7.1. T-model of one phase line with currents and voltages marked

We define the H-matrix to satisfy the following equation:

$$\begin{bmatrix} \hat{U}_2 \\ \hat{I}_2 \end{bmatrix} = \hat{H} * \begin{bmatrix} \hat{U}_1 \\ \hat{I}_1 \end{bmatrix} \qquad (7.1)$$

When solving circuit equations without admittance voltage we get the following result:

$$\hat{H} = \begin{bmatrix} 1 + \dfrac{\hat{Y}*\hat{Z}}{2} & \hat{Z} + \dfrac{\hat{Y}*\hat{Z}^2}{2} \\ \hat{Y} & 1 + \dfrac{\hat{Y}*\hat{Z}}{2} \end{bmatrix} \qquad (7.2)$$

7.2 H-matrix subdivisions

When there is a large number of conductors the computations required to solve standard H matrix is too high, however if the H matrix is split into individual parts then the computations are much easier. This is done by not taking into account the whole of the T model at once but by subdividing it into 3 matrices: the Y matrix and 2 Z matrices. After calculating each matrix individually then by using dot product on the matrices in the correct order you once again get the same H-matrix. The subdivisions are made in such a way that:

$$H - matrix = Zmatrix \,.Ymatrix \,.Zmatrix \qquad (7.3)$$
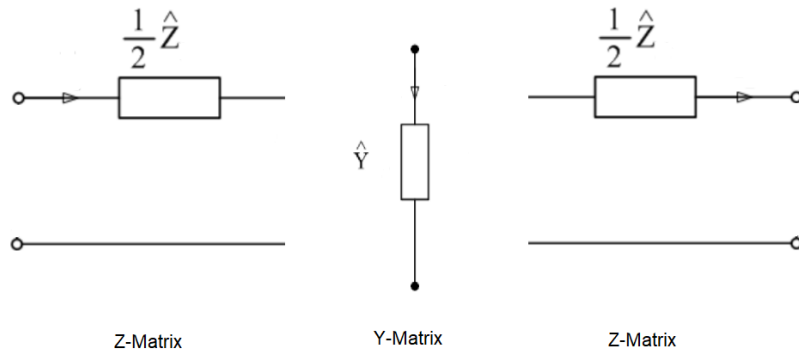
Fig.7.2. Visual representation of the divisions of H-matrix into Z-matrix and Y-matrix

7.3 H-matrix segmentation and fault localization

H-matrices are rather versatile due to the nature of how they segment and cascade those segments. Cascading 2 H-matrices where the output of the first matrix (denoted by 1) is the input for the second matrix (denoted by 2) and the output of the second matrix is the final value (denoted by 3) the equation (7.3) shown below holds.

$$\begin{bmatrix} \hat{U}_3 \\ \hat{I}_3 \end{bmatrix} = \hat{H} * \begin{bmatrix} \hat{U}_2 \\ \hat{I}_2 \end{bmatrix} = \hat{H}^2 * \begin{bmatrix} \hat{U}_1 \\ \hat{I}_1 \end{bmatrix} \qquad (7.4)$$

This can be used to cascade as many H-matrices as needed to the nth power.
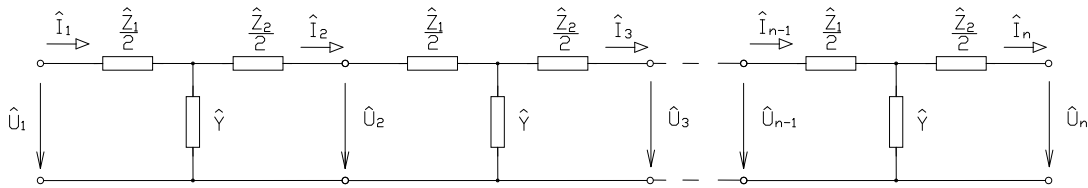
Fig.7.3. Cascaded n H-matrices

If we consider infinitely small sections which are then cascaded the difference between the wave description of the line and the lumped parameters such as the telegraph equation disappears. This is a method of solving the telegraph equation. If we also take into account the properties of matrix rooting, then once we have the parameters of the entire line one can segment the line as needed.

16

To segment an H-matrix into X parts, simply apply an inverse power of X to the H-matrix as so: $\widehat{H}^{\frac{1}{X}}$. This is done with the function "MatrixPower[]". This enables the segmentation of an entire overhead line and then by cascading segment by segment we can apply the H-matrix to any point on the overhead line.

For example applying the H-matrix at the nth segment of the line and the line is divided into m segments it would look like this:

$$\begin{bmatrix} \widehat{U}_n \\ \widehat{I}_n \end{bmatrix} = \widehat{H}^{\frac{m-n}{m}} * \begin{bmatrix} \widehat{U}_1 \\ \widehat{I}_1 \end{bmatrix} \qquad (7.5)$$

The reason we want to apply the H-matrix on specific segments of the overhead line is to be able to accurately represent faults when they occur. Consider a fault occurring at the mth segment of the overhead line. Then the H-matrix is divided into 3 sections:

$$\widehat{H}^m . \widehat{H}^{Fault} . \widehat{H}^{n-m-1} = \widehat{H}^{\frac{m-n}{m}} \qquad (7.6)$$

$$\begin{bmatrix} \widehat{U}_n \\ \widehat{I}_n \end{bmatrix} = \widehat{H}^m . \widehat{H}^{Fault} . \widehat{H}^{n-m-1} * \begin{bmatrix} \widehat{U}_1 \\ \widehat{I}_1 \end{bmatrix} \qquad (7.7)$$
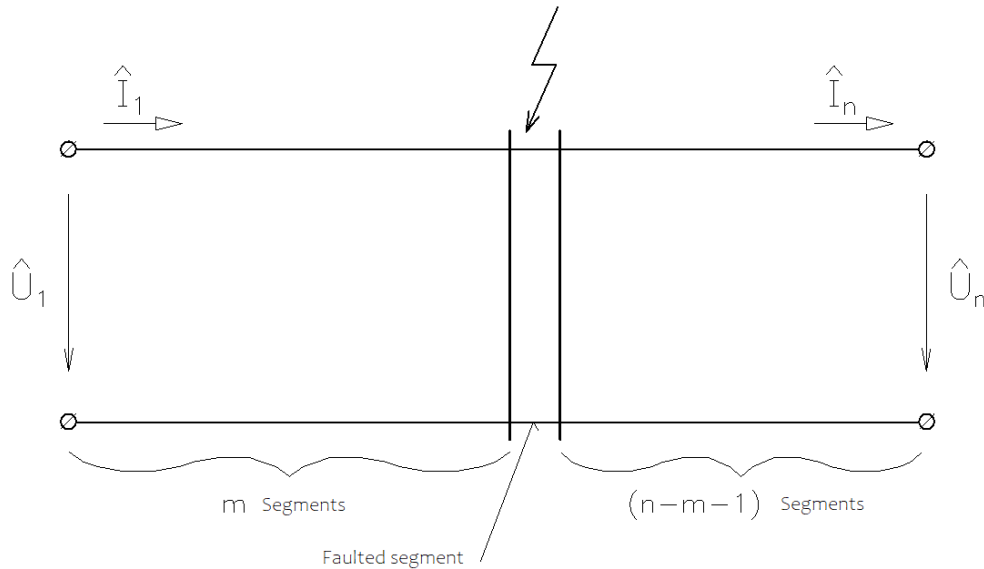
Fig.7.4. Visual representation of the H-matrix formula (7.7).

In real life situation the position 'm' would not be known and the type fault matrix must be determined beforehand. The $\widehat{H}^{Fault}$ is determined by taking into account the type of fault we are

dealing with as will be discussed in chapter 8. Once we find the $\hat{H}^{Fault}$ matrix we can solve for the location of the fault.

To solve for the correct 'm' segment, and therefore the location, iterate equation (7.7) over the entire overhead line. Compare the synchrophasors of each iteration of the equation (7.7) with those already known from measurements. By using a 'FindMinimum[]' function on the compared results we can find the most probable location of the fault.

8. Creating Z, Y and H matrices based on type of fault

The previous chapter covered the H-matrix theory but this chapter covers a more detailed procedure for subdividing the H-matrix and the creation of the fault H-matrix from equation (7.7)

8.1 Z-matrix

To create the Z-matrix the following equations were solved using the 'CoefficientArrays[]' function for all uIn and iIn:

$$\sum_i^n [\text{uOut}_i == \text{uIn}_i - \sum_j^n [\text{iIn}_i Z_{j,i}]] \qquad (8.1)$$

$$\sum_i^n [\text{iOut}_i == \text{iIn}_i] \qquad (8.2)$$

Where n is the number of conductors [-], uOut/uIn are voltages [V], iOut/iIn are currents [A] and Z is the impedance [Ω] at the respective position. These equations were made from the fig.8.1 and extrapolated for multiple conductors and their mutual inductance. It should be mentioned that every impedance (Z) in the equations was already halved unlike the figure shows.
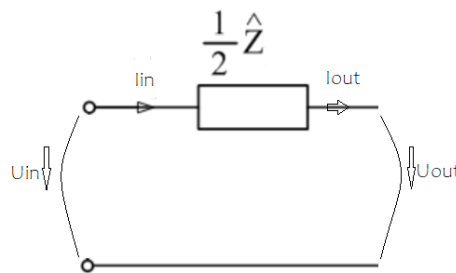
Fig.8.1. The impedance portion of the H-matrix.

8.2 Y-matrix

To create the Y-matrix the following equations were solved using the 'CoefficientArrays[]' function for all uIn and iIn:

$$\sum_i^n iOut_i == iIn_i - Y0_i * uIn_i - \sum_j^n [Y_{i,j} * (uIn_i - uIn_j)] \qquad (8.3)$$

$$\sum_i^n [uOut_i == uIn_i] \qquad (8.4)$$

Where n is the number of conductors [-], uOut/uIn are voltages [V], iOut/iIn are currents [A], Y is the admittance [S] at the respective position and Y0 is the phase to ground admittance [S] at the respective position. These equations were made from the fig.8.2 and extrapolated for multiple conductors and their mutual admittances.
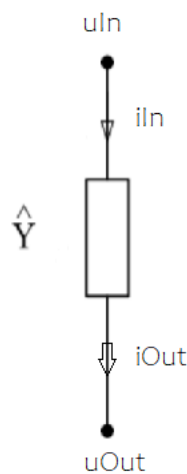
Fig.8.2. The admittance portion of the H-matrix

8.3 H-matrix of fault

An H-matrix of a fault depends on the type of fault that occurred. Every fault has a different matrix and conditions. Since the fault is of no length then it has no impedance or admittance except for the location of the fault. Therefore this matrix has only non-zero variables on the parts of the line that are faulty. It should also be mentioned that since the procedure requires a dot product between this matrix and another matrix like in equation (7.7) there is a requirement for the H-matrix of fault to be an identity matrix with also including the fault variables. It should be noted that although only admittances of faults are shown, the matrices shown are results of Z-matrix dot product with Y-matrix

and then dot product with another Z-matrix. This is the reason for the matrices having a distinct quarter for the fault admittances.

The 'RofFault' shown in graphical representation of the H-matrices of fault below are the resistance of the fault. The reason for choosing only a resistive character for the fault is due to the way electric arcs were modelled. The fault characteristics are slightly different in regards to which type of fault occurs [8]. However to keep the homogeneity, when studying the accuracy of the H-matrix method for fault localization, an average resistance of 20Ω was chosen.

Phase-to-ground fault

For phase-to-ground faults the fault matrix will have only phase to ground admittance ($Y0_x$) of the faulted phase as a non-zero variable. An example of the matrix is shown in pic 8.3. For the graphical representation a smaller 3 phase overhead line was used and the fault was placed at the phase number 2.

$$\begin{bmatrix} 1 & 0 & 0 & 0 & 0 & 0 \\ 0 & 1 & 0 & 0 & 0 & 0 \\ 0 & 0 & 1 & 0 & 0 & 0 \\ 0 & 0 & 0 & 1 & 0 & 0 \\ 0 & -\dfrac{1}{\text{RofFault}} & 0 & 0 & 1 & 0 \\ 0 & 0 & 0 & 0 & 0 & 1 \end{bmatrix}$$

Fig.8.3. H-matrix of fault for phase-to-ground fault on phase number 2.

Double-phase-to-ground fault

Similarly as in the phase-to-ground fault the phase to ground admittance ($Y0_x$) is going to be a non-zero variable but also we have phase to phase admittances that are non-zero. The phase to phase admittances depend on which of the phases have come into contact. If phase 1 and 2 are faulty then the mutual admittances $Y_{1,2}$ and $Y_{2,1}$ as well as the phase to ground admittances $Y0_1$ and $Y0_2$ are non-zero variables. A graphical representation is shown in the fig.8.4.

$$\begin{bmatrix} 1 & 0 & 0 & 0 & 0 & 0 \\ 0 & 1 & 0 & 0 & 0 & 0 \\ 0 & 0 & 1 & 0 & 0 & 0 \\ -\dfrac{3}{\text{RofFault}} & \dfrac{2}{\text{RofFault}} & 0 & 1 & 0 & 0 \\ \dfrac{2}{\text{RofFault}} & -\dfrac{3}{\text{RofFault}} & 0 & 0 & 1 & 0 \\ 0 & 0 & 0 & 0 & 0 & 1 \end{bmatrix}$$

Fig.8.4. H-matrix of fault for a double-phase-to-ground fault on phases number 1 and 2.

Phase-to-phase fault

In phase-to-phase faults matrix we only have the faulted phases admittances. If phases 1 and 2 are in contact then the admittances $Y_{1,2}$ and $Y_{2,1}$ are non-zero. A graphical representation is shown in fig.8.5.

$$
\begin{bmatrix}
1 & 0 & 0 & 0 & 0 & 0 \\
0 & 1 & 0 & 0 & 0 & 0 \\
0 & 0 & 1 & 0 & 0 & 0 \\
-\dfrac{2}{\text{RofFault}} & \dfrac{2}{\text{RofFault}} & 0 & 1 & 0 & 0 \\
\dfrac{2}{\text{RofFault}} & -\dfrac{2}{\text{RofFault}} & 0 & 0 & 1 & 0 \\
0 & 0 & 0 & 0 & 0 & 1
\end{bmatrix}
$$

Fig.8.5. H-matrix of fault for a phase-to-phase fault on phases number 1 and 2.

Three-phase-to-ground fault

The three phase fault has symmetric admittances over all 3 phases. All phases have an equal admittance and the resulting matrix is shown in the fig.8.4.

$$
\begin{bmatrix}
1 & 0 & 0 & 0 & 0 & 0 \\
0 & 1 & 0 & 0 & 0 & 0 \\
0 & 0 & 1 & 0 & 0 & 0 \\
-\dfrac{3}{\text{RofFault}} & \dfrac{1}{\text{RofFault}} & \dfrac{1}{\text{RofFault}} & 1 & 0 & 0 \\
\dfrac{1}{\text{RofFault}} & -\dfrac{3}{\text{RofFault}} & \dfrac{1}{\text{RofFault}} & 0 & 1 & 0 \\
\dfrac{1}{\text{RofFault}} & \dfrac{1}{\text{RofFault}} & -\dfrac{3}{\text{RofFault}} & 0 & 0 & 1
\end{bmatrix}
$$

Fig.8.6. H-matrix of three-phase-to-ground fault.

9. Mathematical model

To create a mathematical model of overhead lines a software is required, I chose Mathematica® version 12.0.

The mathematical model consists of 2 parallel lines. Which consist of 6 phase conductors and 2 earthing lines, which equals to a total of 8 conducting lines. The modelled lines are between two substations. The mathematical model must simulate the parameters of these lines in both steady state and when transient events occur.
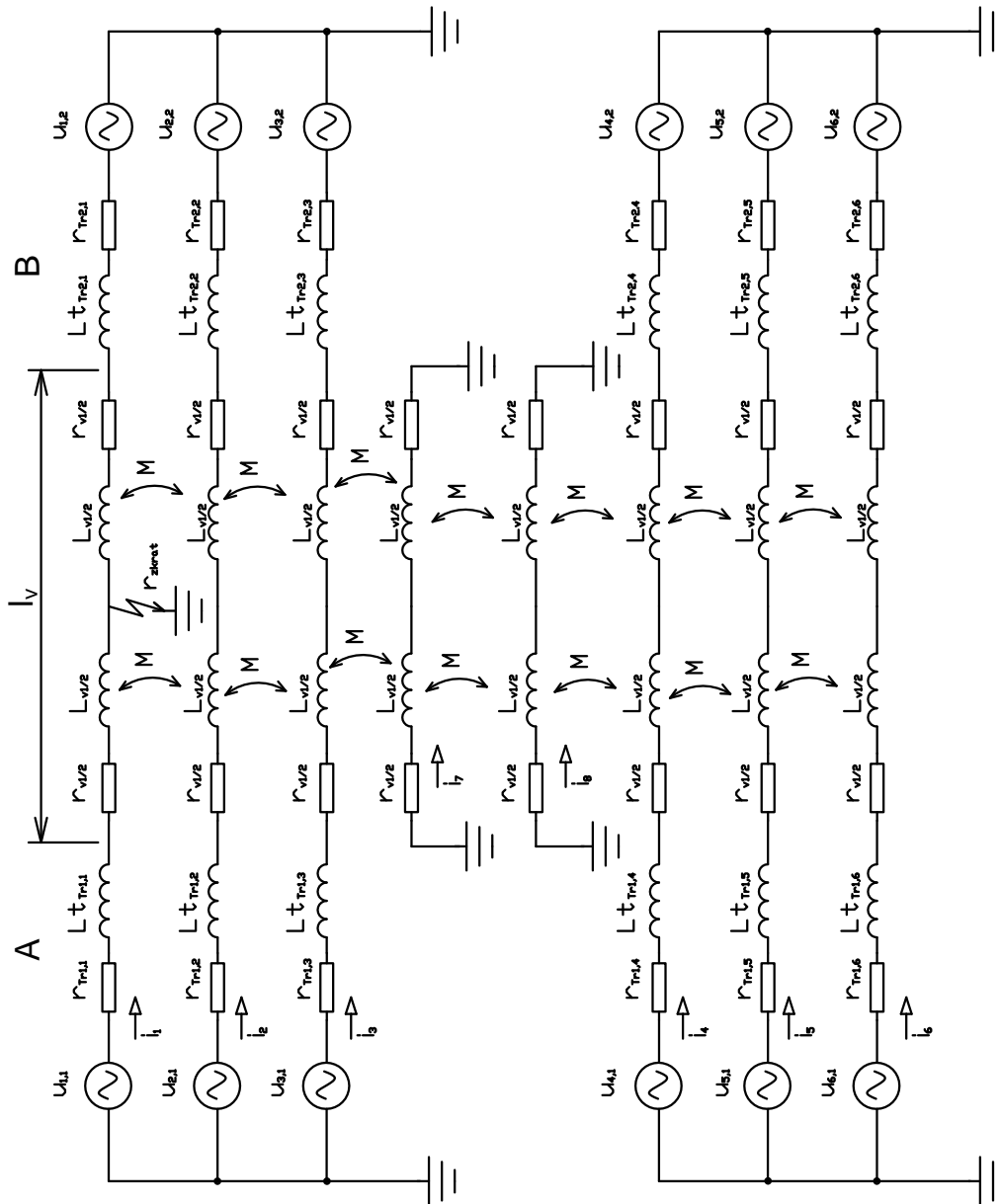
Fig.9.1. Complete wire configuration.

Fig.9.1 shows the entire wiring diagram between the two substations A and B where the length between them is indicated by lv. Mutual inductances by the lines are represented by M, it would be impractical to show all the mutual inductances and therefore only the adjacent inductions are shown but all of the necessary inductances were taken into account when calculating the models. All variables denoted with 'Tr1-6' are simply parameters of the respective transformers. On the other hand all other variables are parameters of their respective lines.

9.1 Dimensions and parameters of lines

A very important aspect is the dimensioning of the overhead lines. This affects all types of mutual interactions between the lines. The dimensions of the lines can be seen in Table 3 below and a visual representation of the overhead lines is depicted in fig.9.2.

	Phase (1)		Phase (2)		Phase (3)		Ground line (7)	
1st Line	Δ x (m)	y (m)	Δ x (m)	Δ y (m)	Δ x (m)	Δ y (m)	Δ x (m)	Δ y (m)
	-10,7	31	-14,5	19,5	-7,5	19,5	-6	41
	Phase (4)		Phase (5)		Phase (6)		Ground line (8)	
2nd Line	Δ x (m)	Δ y (m)	Δ x (m)	Δ y (m)	Δ x (m)	Δ y (m)	Δ x (m)	Δ y (m)
	10,7	31	14,5	19,5	7,5	19,5	6	41

Table 3. The dimensions of the overhead lines
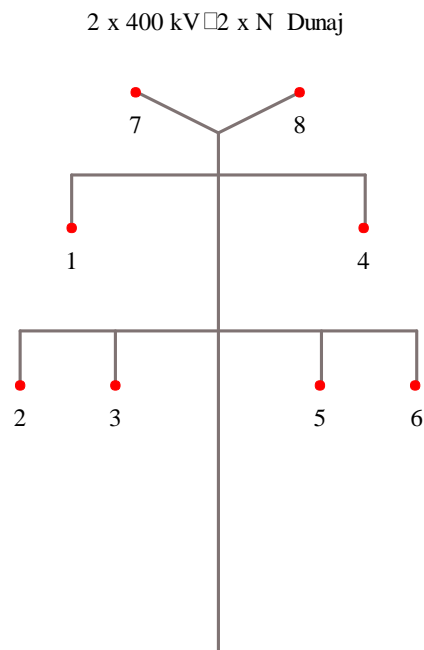
2 x 400 kV □2 x N Dunaj

Fig.9.2. Dunaj type of overhead line mast.

9.2 Stead state model

Steady state condition refers to the periodic nature of the state. Periodicity is an expression of a repeating value or pattern. So in our case this state is when there is no change in either the input or

output values for some time and most importantly no changes to the impedance and admittances of the wires during that time. This state was modelled by the following equation:

$$u(t) = U_m * \sin(\omega t + \varphi) \qquad (9.1)$$

Where u(t) is the instantaneous voltage value (V), U_m is the amplitude (V), ω is the angular frequency (rad* s^{-1}) and φ is the phase angle (rad). From these sinusoidal waves of voltage we acquire their phasor values respectively.
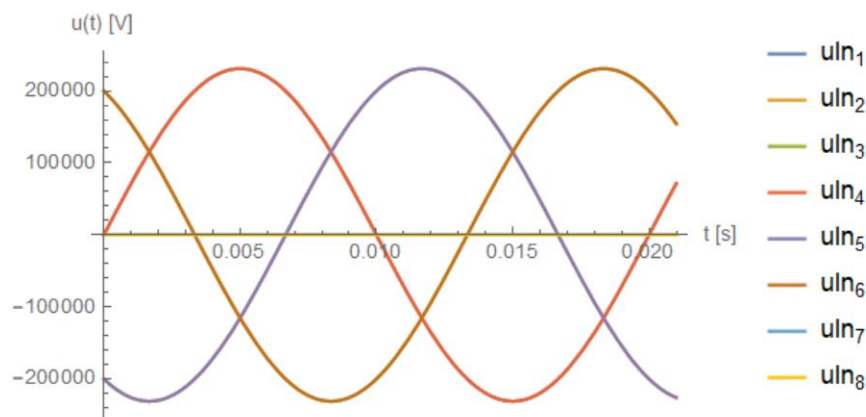

Fig.9.3. 3-Phase voltage model from Mathematica® (not all phases are visible since they overlap)

9.3 Transient state

Usually another set of equations would model the transient state however we can immediately use the H-matrix in a way such as described in equation (7.5). Since we are the ones simulating the fault, we can choose the unknown variable m and impedance of the fault. This means that we effectively model a faulted overhead line using H-matrices and there is no need for equations and considerations of d-c components. When solving the transient state using H-matrix we directly get the vector forms of the synchrophasors for current and voltage.

Considering these are real lines a load is usually present at the end of the line as consumers. We consider this load to be 300 MW with a power factor of 0.95.

$$Zload = \frac{400^2}{300*10^6}(1 - i * \text{Tan}[0.95]) \qquad (9.2)$$

This load permits us to establish another set of equations:

$$\sum_i^n [\text{iOut}_i * Zload == \text{uOut}_i] \qquad (9.3)$$

24

This set of equations combined with H-matrix of fault from chapter 8 and knowing the values of the uIn$_x$ phasors Considering these are real lines a load is usually present at the end of the line as consumers. We consider this load to be 300 MW with a power factor of 0.95.

$$Zload = \frac{400^2}{300 * 10^6}(1 - i * \text{Tan}[0.95]) \qquad (9.2)$$

This load permits us to establish another set of equations:

$$\sum_i^n [\text{iOut}_i * Zload == \text{uOut}_i] \qquad (9.3)$$

This set of equations combined with H-matrix of fault from chapter 8 and knowing the values of the uIn$_x$, phasors iOut$_i$ and uOut$_i$ can be solved using the Mathematica® formula 'Solve[]'.

10. H-matrix algorithm results

An important aspect of the H-matrix method is that it delivers accurate results with a finite algorithm. Testing the extent of this accuracy is a crucial part of developing this algorithm. Firstly the algorithm was run with so called "perfect phasors". Meaning that the phasors were perfect sinusoidal waves and also there was no inaccuracy when reading the phasors. These were the ideal conditions for the algorithm. However this does not represent real life situations. Further testing with errors introduced to all the phasors needed to calculate the results were introduced. As discussed in chapter 5, the synchrophasors had limitations to their respective inaccuracies. 1% of the TVE only was allowed (even though the recommended amount is lower but we assume a worst case scenario).

Out of the rule for 1% TVE four worst cases were assumed. The four cases consisted of the minimum and maximum of the phasor magnitude error equal to 1% and the minimum and maximum of the phasor angle equal to 1%.

Test 1	Test 2	Test 3	Test 4
+ 1% phase angle	-1% phase angle	+1% magnitude	-1% magnitude

Table 10.1. The names given to each test case

Another basis that needed to be tested in algorithms that deal with distribution is the effect the distance where the fault occurs has. For that we tested each of the four fault types on each of the four worst case scenarios at 25%, 50% and 75% of the length of the overhead line respectively.

Since we do not know in which phase the fault has occurred the H-matrix algorithm tests all possible phases in a similar way as described in chapter 7. Then the choice of the correct phase is made by checking which phase has the minimum difference between the calculated H-matrix and the actual H-matrix.

10.1 Perfect phasor accuracy

The algorithm predicted the fault location segment correctly for every fault type and fault distance when provided with the ideal phasors. However this only means that when given ideal phasors the algorithm has an accuracy of +/- 0.0005 when it comes to the accuracy of fault location. This is due to the choice of segments and the length of the line. We chose 2000 segments with the length of the line 100km. This translates to each segment being 50m. The algorithm was able to choose exactly which segment there was a fault when presented with ideal phasors.

However testing of the perfect phasors is still crucial as it gives indication of the accuracy of the algorithm in terms of difference between the calculated H-matrix and the actual H-matrix. While this does not represent real life situation it does indicate how the algorithm handles each of the four different types of faults.

Perfect phasors	ph-gr	ph-ph	2ph-gr	3-ph
Fault at 400	0.000566541	0.000408405	0.000827	0.000236
Fault at 1000	0.0248028	0.00185744	0.012096	0.002627
Fault at 1600	0.206794	0.006432	0.174779	0.008026

Table 10.2. Actual errors at different fault lengths for all four types of faults.
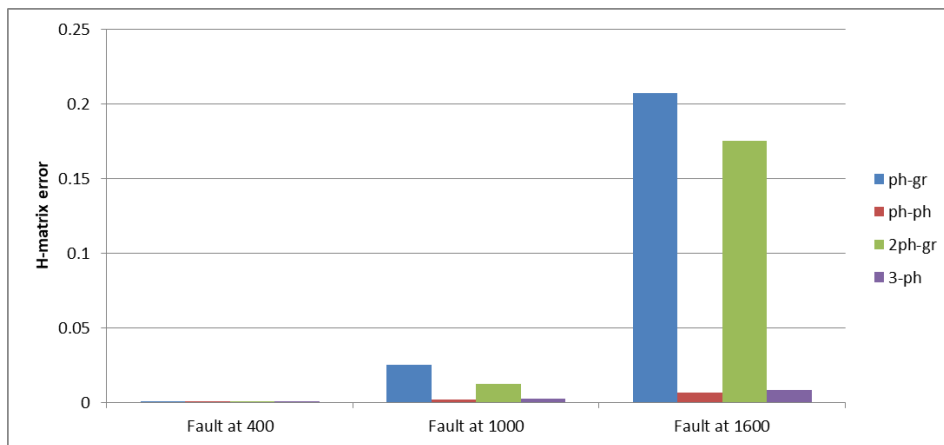

Fig.10.1 Actual errors at different fault lengths for all four types of faults.

The 'actual error' referred to in the previous figure and table was calculated as the difference between the calculated H-matrix and the actual H-matrix we simulated. It should be noted that this graph only puts into perspective the difference between the fault types and their respective fault distance.

The faults phase-to-ground (ph-gr) and double-phase-to-ground (2ph-gr) seem to have the largest errors amongst the four types. It seems that the influences of the ground parameters are important in the algorithm. The fault distance also plays a factor with higher errors appearing with longer distances.

10.2 Phase-to-ground fault results

26

The phase-to-ground fault is the fault that most likely occurs in distribution systems [10]. Results for the ideal phasors were perfect when it came to accurately pinpointing the position of the fault. However that is not a real life situation. Testing for all cases for the type of fault ground-to-phase is shown below.

Firstly the algorithm is run through all the phases to test which phase is the faulty one.
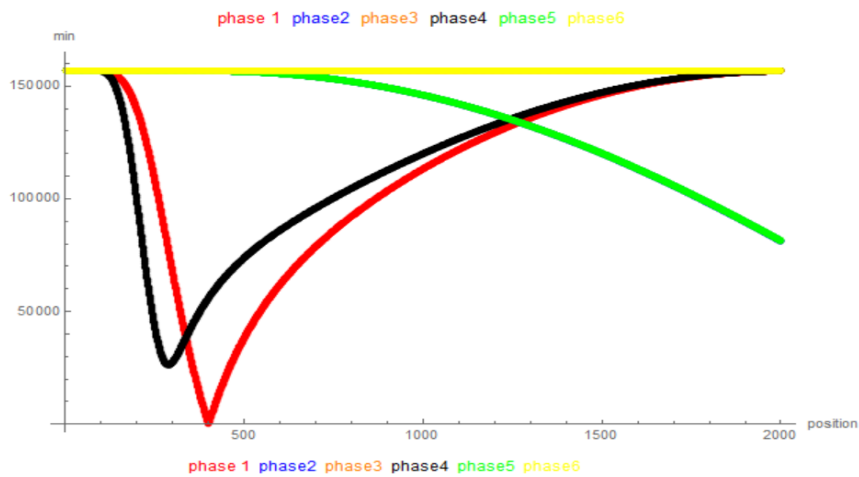

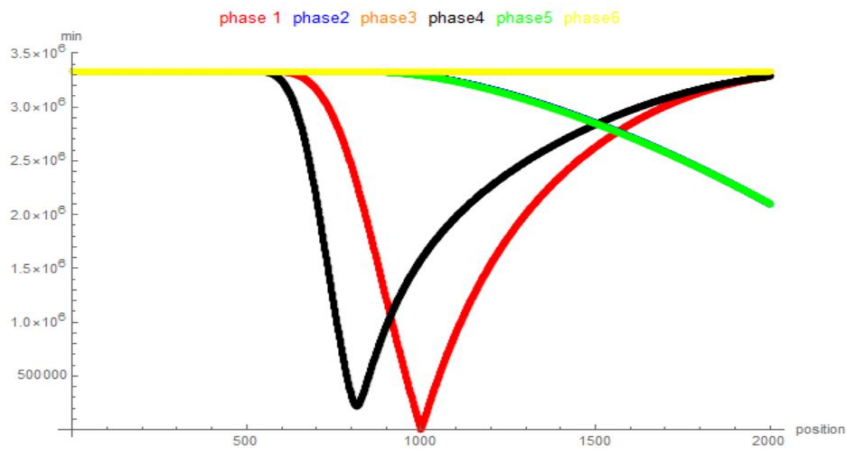Fig.10.2. Phase-to-ground fault at segment 400.

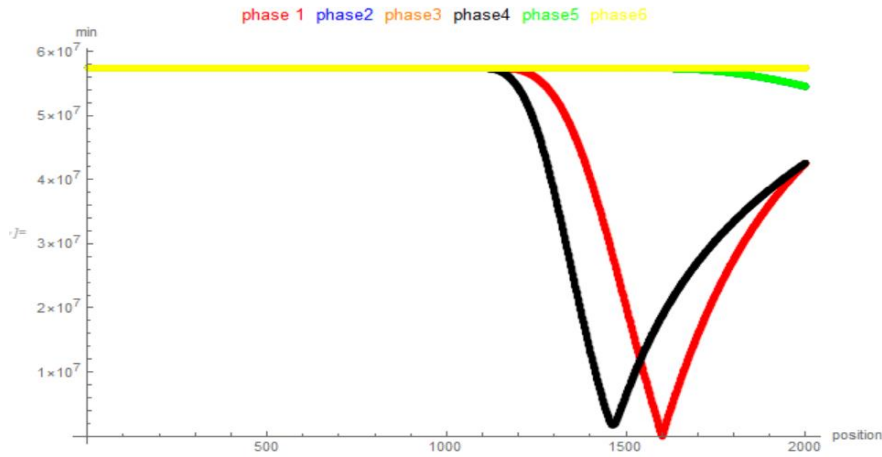Fig.10.3 Phase-to-ground fault at segment 1000.

Fig.10.4. Phase-to-ground fault at segment 1600.

The previous graphs show the difference between the H-matrix that was calculated with the actual H-matrix on the Y axis (min) and the respective position of the calculated H-matrix.

The algorithm clearly shows that phase 1 is the phase that has the fault. The difference between the second closest candidate (phase 4) is several orders ($\sim 10^6$) of magnitude larger. It should be noted that some phases do not show as they overlap however mainly on the top of the graph and no overlap occurs with the phase 1.

Table 10.2 shows the algorithm results of phase 1.

fault at position: 400	calculated position	calculated distance	error in percentage	error in metres
perfect phasors	400	20000	0	0
test 1	416	20800	0.8	800
test 2	383	19150	0.85	850
test 3	410	20500	0.5	500
test 4	390	19500	0.5	500
fault at position: 1000	calculated position	calculated distance	error in percentage	error in metres
perfect phasors	1000	50000	0	0
test 1	1007	50350	0.35	350
test 2	994	49700	0.3	300
test 3	1006	50300	0.3	300
test 4	994	49700	0.3	300
fault at position: 1600	calculated position	calculated distance	error in percentage	error in metres
perfect phasors	1600	80000	0	0
test 1	1604	80200	0.2	200
test 2	1596	79800	0.2	200
test 3	1603	80150	0.15	150
test 4	1597	79850	0.15	150

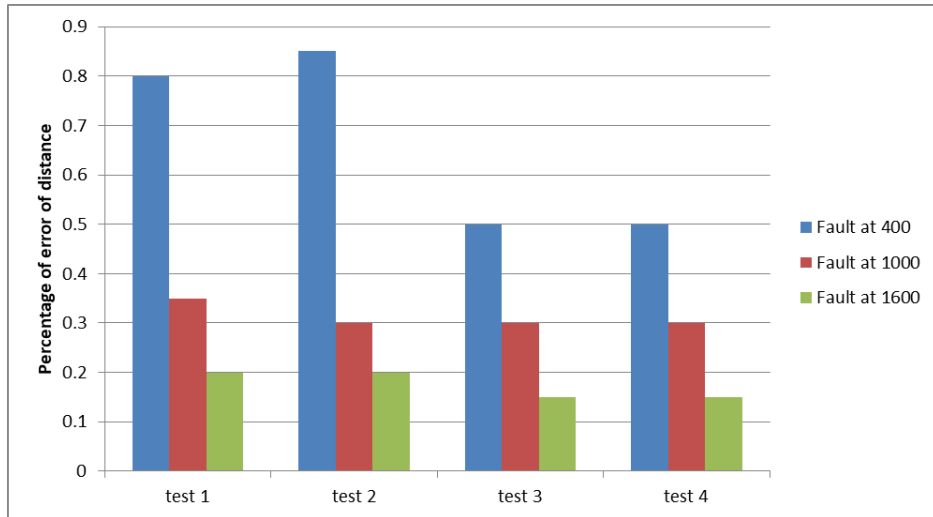Table 10.3. Results of phase-to-ground fault.

Fig.10.5. The percentage of error compared with the fault distance and type for ph-gr fault.

10.3 Phase-to-phase fault results

The faulty phases were chosen to be phases 4 and 6. From the figures below it is clearly seen that the algorithm correctly assessed this.
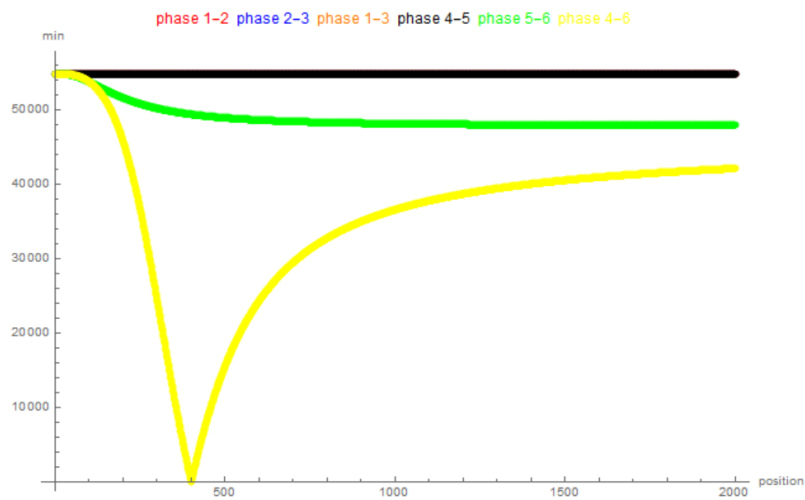

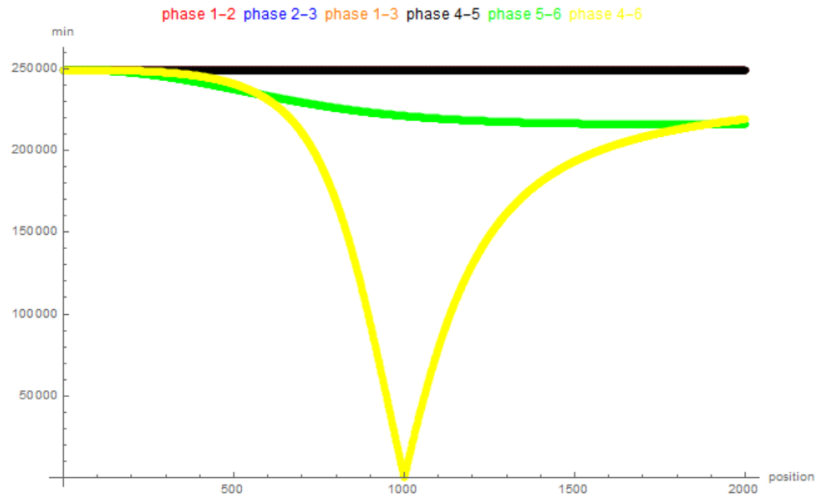Fig.10.6. phase-to-phase fault results at position 400.

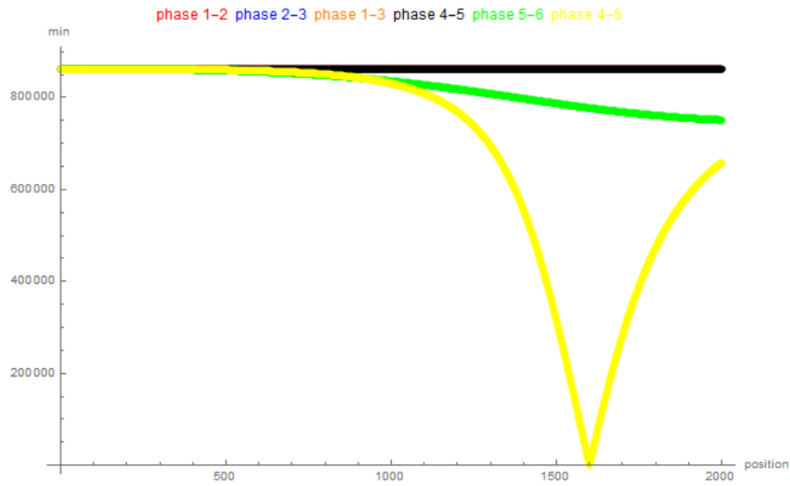Fig.10.7. phase-to-phase fault results at position 1000.

Fig.10.8. phase-to-phase fault results at position 1600.

The previous graphs show the difference between the H-matrix that was calculated with the actual H-matrix on the Y axis (min) and the respective position of the calculated H-matrix.

fault at position: 400	calculated position	calculated distance	error in percentage	error in metres
perfect phasors	400	20000	0	0
test 1	425	21250	1.25	1250
test 2	377	18850	1.15	1150
test 3	408	20400	0.4	400
test 4	393	19650	0.35	350
fault at position: 1000	calculated position	calculated distance	error in percentage	error in metres
perfect phasors	1000	50000	0	0
test 1	1008	50400	0.4	400
test 2	992	49600	0.4	400
test 3	1009	50450	0.45	450
test 4	991	49550	0.45	450
fault at position: 1600	calculated position	calculated distance	error in percentage	error in metres
perfect phasors	1600	80000	0	0
test 1	1604	80200	0.2	200
test 2	1596	79800	0.2	200
test 3	1603	80150	0.15	150
test 4	1603	80150	0.15	150

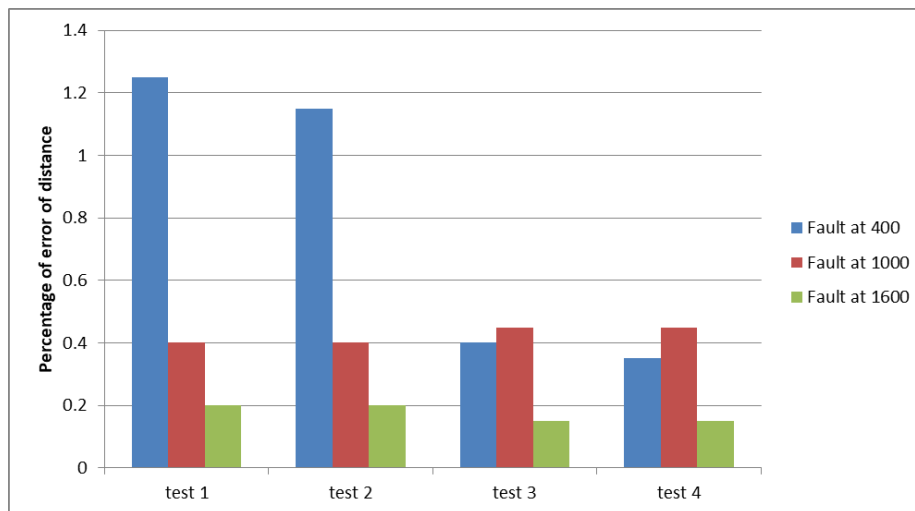Table 10.4 Results of phase-to-phase fault.

Fig.10.9. The percentage of error compared with the fault distance and type for ph-ph fault.

10.4 Double-phase-to-ground fault results

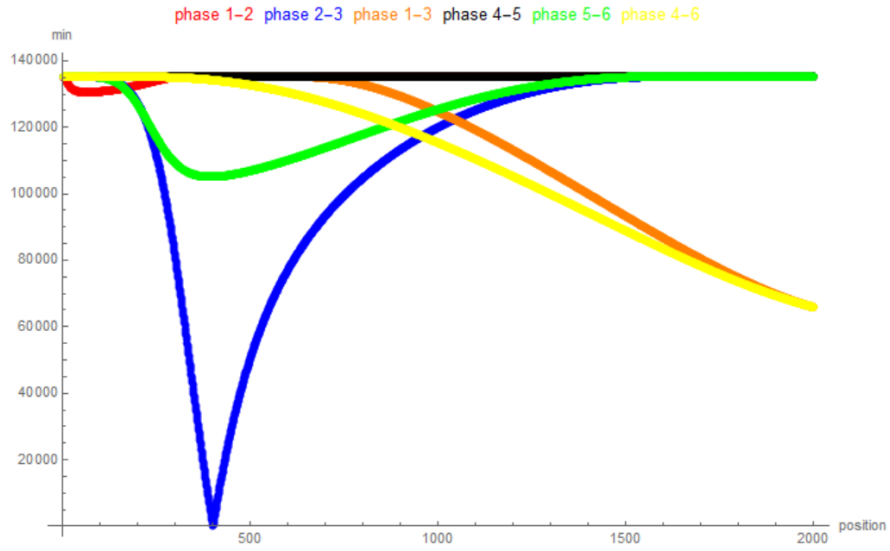The faulty lines were chosen to be phases 2 and 3 with a short circuit to the ground.

Fig.10.10. double-phase-to-ground fault results at position 400.
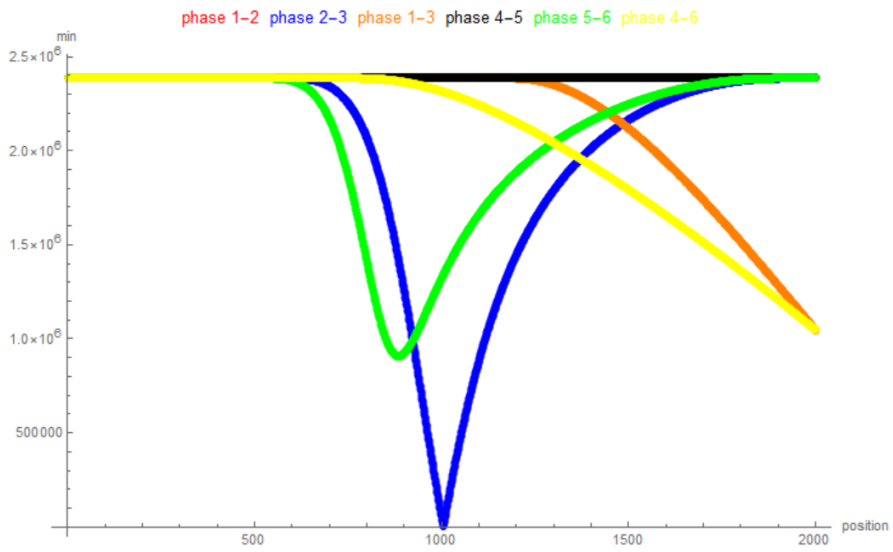

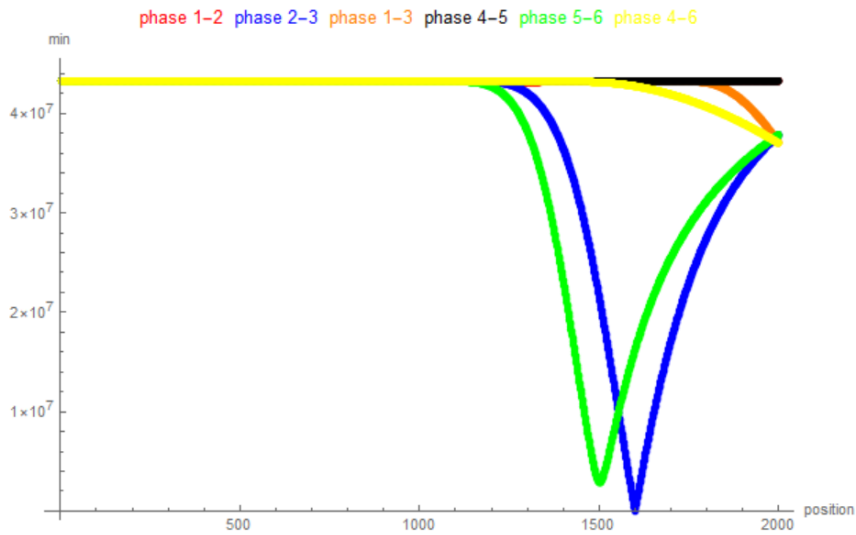Fig.10.11. double-phase-to-ground fault results at position 1000.

Fig.10.12. double-phase-to-ground fault results at position 1600.

It should be noted that on the third graph (figure 10.9) the difference between the phases 2-3 and phases 5-6 was still in the order of ~10^6 larger.

fault at position: 400	calculated position	calculated distance	error in percentage	error in metres
perfect phasors	400	20000	0	0
test 1	412	20600	0.6	600
test 2	388	19400	0.6	600
test 3	410	20500	0.5	500
test 4	390	19500	0.5	500
fault at position: 1000	calculated position	calculated distance	error in percentage	error in metres
perfect phasors	1000	50000	0	0
test 1	1004	50200	0.2	200
test 2	996	49800	0.2	200
test 3	1006	50300	0.3	300
test 4	994	49700	0.3	300
fault at position: 1600	calculated position	calculated distance	error in percentage	error in metres
perfect phasors	1600	80000	0	0
test 1	1603	80150	0.15	150
test 2	1597	79850	0.15	150
test 3	1603	80150	0.15	150
test 4	1597	79850	0.15	150

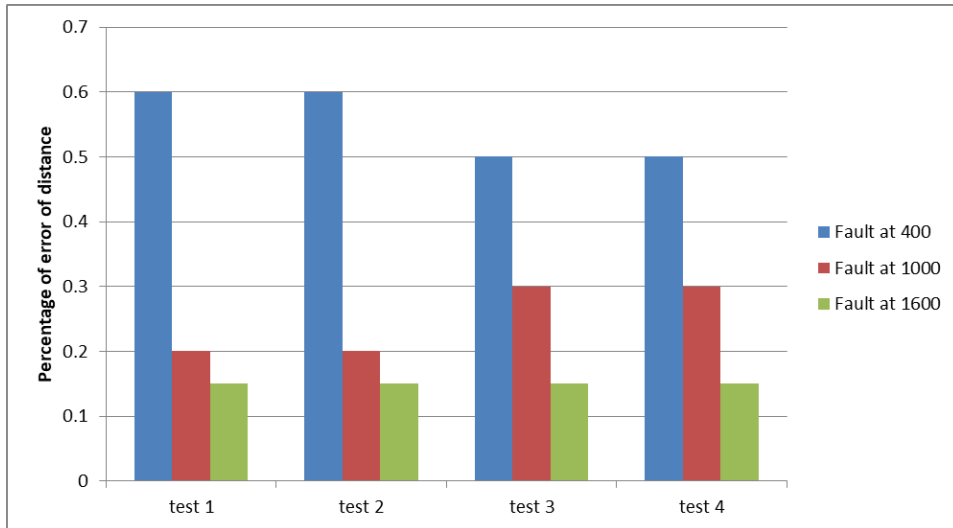Table 10.5 Results of phase-to-phase fault.

Fig.10.13. The percentage of error compared with the fault distance and type for 2-ph-grd fault.

10.5 Three-phase fault results
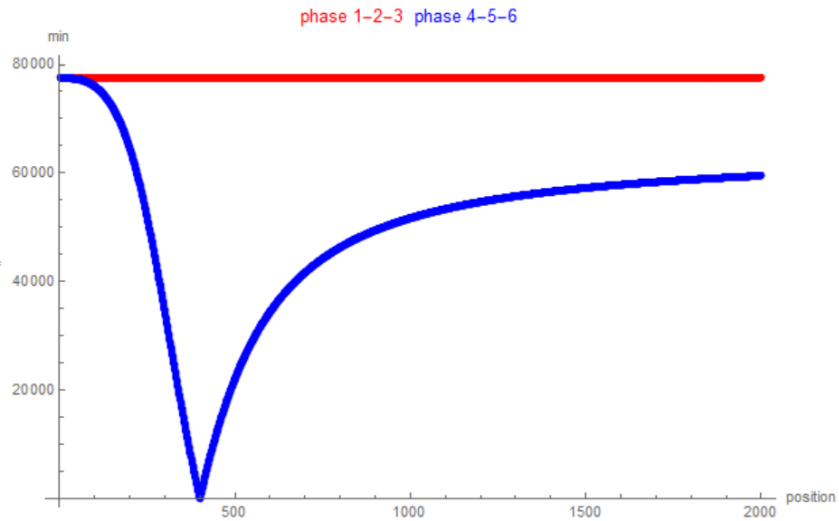
The faulty phases were chosen to be 4,5 and 6.

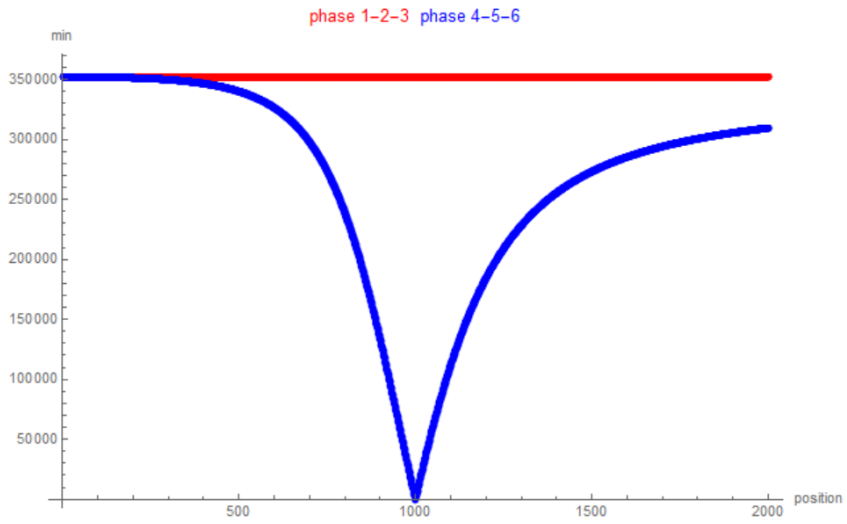Fig.10.14. three-phase fault results at position 400.

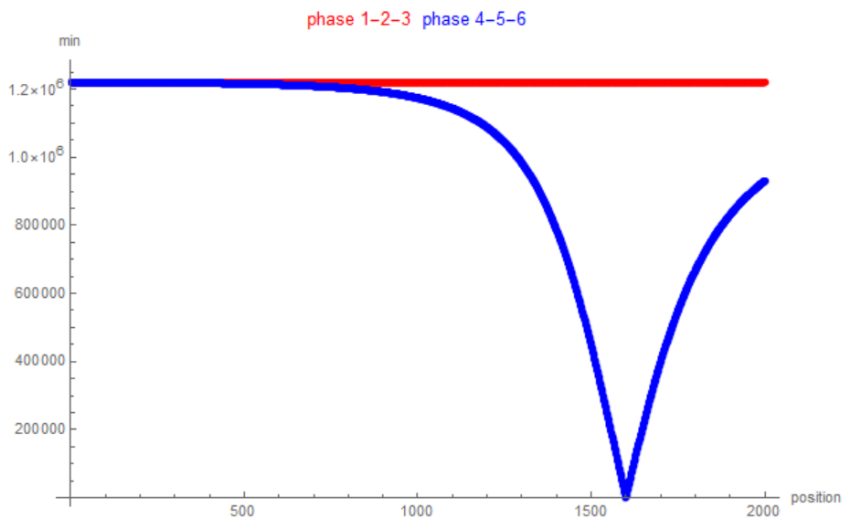Fig.10.15.Three-phase fault results at position 1000.

Fig.10.16. three-phase fault results at position 1600.

fault at position: 400	calculated position	calculated distance	error in percentage	error in metres
perfect phasors	400	20000	0	0
test 1	425	21250	1.25	1250
test 2	377	18850	1.15	1150
test 3	408	20400	0.4	400
test 4	393	19650	0.35	350
fault at position: 1000	calculated position	calculated distance	error in percentage	error in metres
perfect phasors	1000	50000	0	0
test 1	1008	50400	0.4	400
test 2	992	49600	0.4	400
test 3	1008	50400	0.4	400
test 4	991	49550	0.45	450
fault at position: 1600	calculated position	calculated distance	error in percentage	error in metres
perfect phasors	1600	80000	0	0
test 1	1604	80200	0.2	200
test 2	1596	79800	0.2	200
test 3	1603	80150	0.15	150
test 4	1597	79850	0.15	150

Table 10.6 Results of three-phase fault.

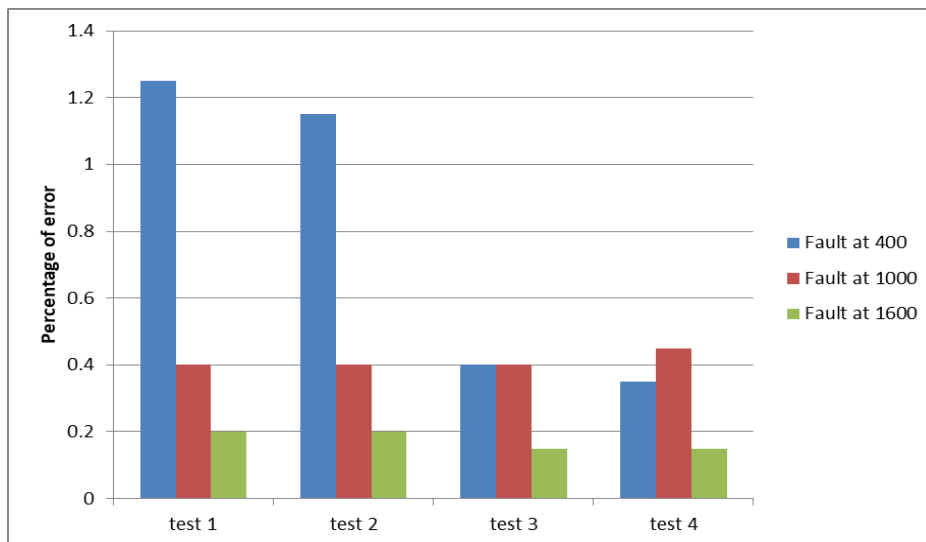

Fig.10.17. The percentage of error compared with the fault distance and type for 3-ph fault.

11. Conclusion

From the results it seems that overall the fault distance plays a major role. The farther the fault location is the better the accuracy. This could be due to the phenomena discussed in the beginning of chapter 6. However this also contradicts the observed behaviour in chapter 10.1.

In chapter 10.1 it was observed that the algorithm handles better shorter distances with ideal phasors however when tested with degrees of errors in the phasors the shorter distance faults have larger errors. This same format where shorter distances give larger errors keeps on appearing at every type of fault.

Also in contradiction to the chapter 10.1, the types of faults that performed better were the faults with short-circuit to the ground. This shows the importance of fully testing an algorithm as counter-intuitive data like this could show up.

It should also be noted that the overall difference between the calculated H-matrix and the actual H-matrix decreases with shorter distance of faults. This makes sense as the actual H-matrix itself is smaller when the distance is shorter.

The graphs shown in figures 2-4, 6-8, 10-12 and 14-16 were all recorded when the algorithm was given perfect phasors. These graphs always show a massive order of magnitude difference between the non-faulty and the faulty phases. However when tested under the worst case scenarios the difference between the faulty and non-faulty phases shrunk. At times the difference was only 1 order of magnitude large (10^1). For example the phase-to-phase fault at position 400. The difference between the actual H-matrix and the calculated H-matrix was around 50,000 when not on the right phases or position and the error was almost zero at the correct position and phase. When this was repeated with errors in the phases, the minimum error for the correct phase and position rose to ~4000.

With all this said, the error of the correct faulty phase was always at least 1 order of magnitude smaller than the rest and this is taking into account the worst case scenarios in regards to the TVE.

The accuracy of the algorithm was fairly high considering the length of the line and the small errors it gave for localization of faults in all worst case scenarios. However there still are multiple factors that could hinder the accuracy of the results shown. Different RFE and FE testing as discussed in chapter 5 should be done on the algorithm to assess the extent of which the accuracy would be affected. Different types of fault resistances should also be assessed and results gathered. Then obviously a combination of all the different aspects should be tested.

References

[1] William Patrick Davis, (2012). Analysis of faults in overhead transmission lines. California State University, Sacramento

[2] Mohamed E. El-Hawary, (2003). Introduction to Electrical Power Engineering. Wiley-IEEE Press

[3] Steven W. Blume, (2007). Electric Power System Basics: For the Nonelectrical Professional. John Wiley & Sons, Inc., Hoboken, New Jersey. Print ISBN:9780470129876.

[4] "IEEE Standard for Synchrophasor Data Transfer for Power Systems," IEEE Std C37.118.2-2011, 2011, Online: http://standards.ieee.org/ findstds/standard/C37.118.2-2011.html [Accessed: March 20 2020]

[5] J. Schlabbach (2005) Short-circuit Currents. The institution of engineering and technology, London, United Kingdom. Print ISBN: 978-0-86341-514-2

[6] Marko Barišić (2001) IEC 60909-0 Short-circuit currents in three-phase a c. systems. International Electrotechnical 3,rue de Varembé Geneva, Switzerland.

[7] David M. Laverty, Member IEEE, H. Kirkham, Fellow IEEE, D John Morrow, Member IEEE, X Liu (2017) Estimation of Goodness of Fit of Synchrophasors during Transient Faults. IEEE. ISBN: 978-1-5386-2212-4.

[8] Virgilio De Andrade, Elmer Sorrentino (2010).Typical expected values of the fault resistance in power systems. IEEE conference paper.

[9] J.D. Sakala, J.S.J. Daka,(2013).General Fault Admittance Method Solution of a Line-to-Line-to-Ground Fault. Australian Journal of Basic and Applied Sciences, ISSN 1991-8178.

[10] http://www.powerwiki.cz/attach/EN2/EN2_pr06_zkraty_EN.pdf. Accessed on the (20-3-2020).